LOCKHEED MARTIN ENERGY RESEARCH LIBRARIES
3 4456 0514708 9

CENTRAL RESEARCH LIBRARY
DOCUMENT COLLECTION

OAK RIDGE NATIONAL LABORATORY
operated by
UNION CARBIDE CORPORATION • NUCLEAR DIVISION
for the
U.S. ATOMIC ENERGY COMMISSION

ORNL-TM-3712

Cy 11

THICKNESS MEASUREMENTS USING EDDY-CURRENT TECHNIQUES

C. V. Dodd and W. A. Simpson, Jr.

OAK RIDGE NATIONAL LABORATORY
CENTRAL RESEARCH LIBRARY
DOCUMENT COLLECTION
LIBRARY LOAN COPY
DO NOT TRANSFER TO ANOTHER PERSON
If you wish someone else to see this document, send in name with document and the library will arrange a loan.

NOTICE This document contains information of a preliminary nature and was prepared primarily for internal use at the Oak Ridge National Laboratory. It is subject to revision or correction and therefore does not represent a final report.

This report was prepared as an account of work sponsored by the United States Government. Neither the United States nor the United States Atomic Energy Commission, nor any of their employees, nor any of their contractors, subcontractors, or their employees, makes any warranty, express or implied, or assumes any legal liability or responsibility for the accuracy, completeness or usefulness of any information, apparatus, product or process disclosed, or represents that its use would not infringe privately owned rights.

ORNL-TM-3712

Contract No. W-7405-eng-26

METALS AND CERAMICS DIVISION

THICKNESS MEASUREMENTS USING EDDY-CURRENT TECHNIQUES

C. V. Dodd and W. A. Simpson, Jr.

MARCH 1972

OAK RIDGE NATIONAL LABORATORY
Oak Ridge, Tennessee 37830
operated by
UNION CARBIDE CORPORATION
for the
U.S. ATOMIC ENERGY COMMISSION

LOCKHEED MARTIN ENERGY RESEARCH LIBRARIES

3 4456 0514708 9

CONTENTS

	Page
Abstract	1
Introduction	1
Thickness Measurements of a Single Conductor	3
Cladding Thickness Measurements	15
Practical Considerations in Test Design	24
Examples of Design and Experimental Results	26
Summary and Conclusions	29

THICKNESS MEASUREMENTS USING EDDY-CURRENT TECHNIQUES

C. V. Dodd and W. A. Simpson, Jr.

ABSTRACT

Eddy currents have been used for many years to measure the thickness of a single conductor and the thickness of one conductor clad on another. By performing a computer analysis of the problem, we have been able to choose the optimum conditions for performing such measurements. Effects of varying thickness, frequency, coil size, conductivity, lift-off (or coil-to-conductor spacing), and coil resistance are discussed. The use of a phase-sensitive eddy-current instrument in performing thickness and clad thickness measurements is emphasized.

INTRODUCTION

In many critical industrial applications today, the performance of a component depends on the thickness of a metal or on the thickness of one metal clad on another. Typical examples of these critical applications are the cladding on a nuclear reactor fuel element, the thickness of an aircraft wing panel, and the thickness of a chemical cannister.

Eddy currents have been successfully used for many years to measure the thickness and cladding thickness of metals. Early instruments used simple bridge circuits operated in a balanced mode and measured the amplitude of the signal as the balance changed.[1,2] Later instruments used bridges operated in an unbalanced mode to reduce the effects of undesirable variables, principally lift-off, the coil-to-conductor spacing. These instruments usually measured either the magnitude or the phase of the unbalance voltage as a function of thickness. At the

---

[1]R. Hochschild, "Electromagnetic Methods of Testing Metals," Progress in Nondestructive Testing, Vol. I, The Macmillan Company, New York, 1959.

[2]R. C. McMaster, Nondestructive Testing Handbook, Vol. II, The Ronald Press Co., 1959.

low frequencies required to penetrate thick sections of good conductors, the coil dc resistance may become as large as the coil impedance. Later instruments developed at Oak Ridge National Laboratory[3,4] have employed a reflection-type probe as shown in Fig. 1. This probe consists of a large driver coil to generate an electromagnetic field and two pickup coils connected in a differential arrangement to measure the changes in this field. In air, the signals developed across the pickup coils cancel. However, when the probe is placed on the metal, a "reflected field" is produced by the metal. This field, which decreases rapidly with distance from the metal, is detected by the front pickup coil (nearest the metal) but not by the rear coil. The magnitude of the signal is a function

[3]C. V. Dodd, "Applications of a Phase-Sensitive Eddy-Current Instrument," Mater. Evaluation 22(6), 260–263 (June 1964).

[4]C. V. Dodd, "A Portable Phase-Sensitive Eddy-Current Instrument," Mater. Evaluation 26(3), 33–36 (March 1968).

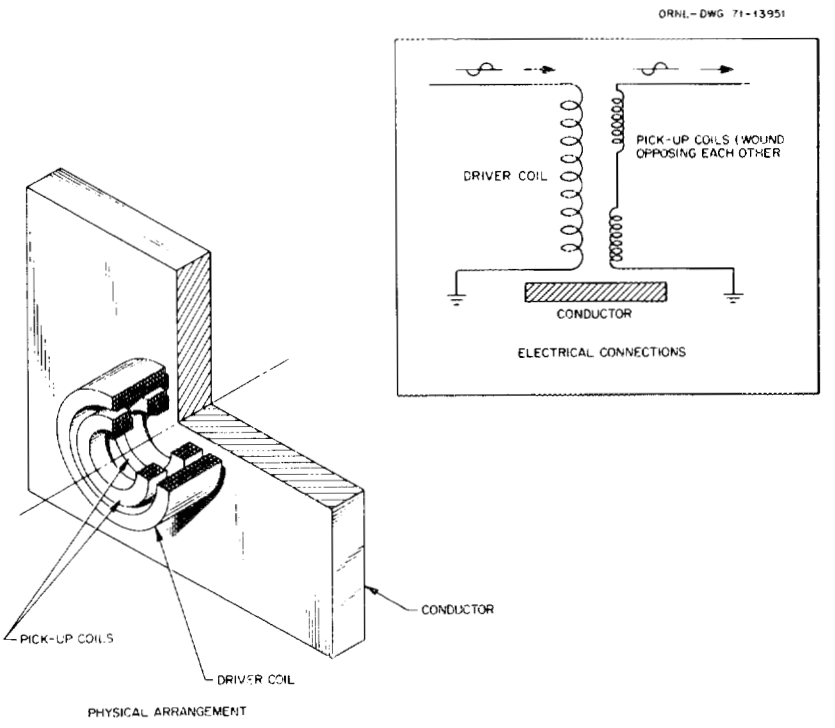

Fig. 1. A Reflection-Type Probe in the Presence of a Conductor.

of the lift-off, but the phase of the signal is relatively insensitive to the lift-off.

This arrangement is equivalent to operating a bridge with a test coil at the sample and a reference coil away from the sample and coupling to them with a single transformer. This type of circuit can be operated at lower frequencies without the effects of variations, which can be caused by ohmic heating, in the coil dc resistance.

Most of the curves given in this report are the result of computer calculations[5] of integral solutions[6] of reflection-type coil problems. Experimental verification of these calculations is given in this report and in other references.[6,7]

THICKNESS MEASUREMENTS OF A SINGLE CONDUCTOR

We shall first consider the case of a reflection-type coil above a single conductor. This represents the most common case of thickness measurements and can be thought of as a special case of cladding thickness with the base material having zero conductivity.

Our first goal is to get the maximum signal (phase shift in our case) for variations from a given nominal thickness. Figure 2 shows how phase shift due to a 10% thickness variation changes as a function of the dimensionless product $\omega\mu\sigma\bar{r}^2$ for coils having various ratios of thickness/coil mean radius (the mean radius, $\bar{r}$, is that of the driver coil). The other symbols, ω, μ, and σ denote the frequency, permeability, and conductivity, respectively. Maximum stability and sensitivity for typical phase-sensitive eddy-current instrumentation are about 0.01° or 1.75×10^{-4} radians. We can see that for each ratio of thickness to coil mean radius there is a value of $\omega\mu\sigma\bar{r}^2$ that gives the maximum phase shift.

---

[5]W. A. Simpson, C. V. Dodd, J. W. Luquire, and W. G. Spoeri, Computer Programs for Some Eddy-Current Problems — 1970, ORNL-TM-3295 (June 1971).

[6]C. V. Dodd, W. E. Deeds, J. W. Luquire, and W. G. Spoeri, Some Eddy-Current Problems and Their Integral Solutions, ORNL-4384 (April 1969).

[7]F. D. Mundt, Eddy-Current Measurements with a Coil Encircling a Two-Conductor Rod, Y-1787 (April 1971).

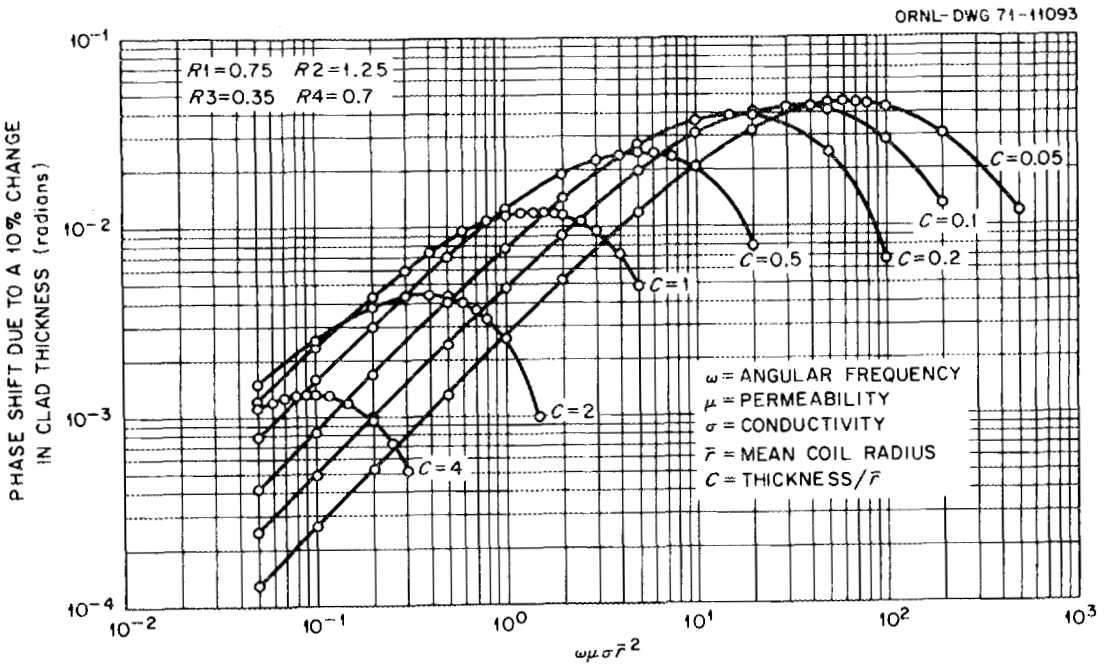

Fig. 2. Phase Shift Due to a 10% Thickness Change Versus $\omega\mu\sigma\bar{r}^2$ for Various Ratios of Thickness/$\bar{r}$. In this and subsequent figures, R1 and R2 represent the normalized inner and outer radii of the driver coil and R3 and R4 the corresponding radii of the pickup coil.

Figure 3 is a plot of this value of $\omega\mu\sigma\bar{r}^2$ for maximum sensitivity and the phase shift at the maximum sensitivity for a 10% thickness change against the ratio of thickness to coil mean radius. Thus, suppose we have a particular inspection problem requiring the measurement of a given nominal thickness of material having a given conductivity, σ, and we have a coil with a given $\bar{r}$. We would first calculate the thickness/$\bar{r}$ ratio and then determine the value of $\omega\mu\sigma\bar{r}^2$ from Fig. 3 that gives the maximum phase shift. Then by knowing this value of $\omega\mu\sigma\bar{r}^2$ and knowing μ, σ, and $\bar{r}^2$, we can calculate the value of frequency ω that will give us the maximum phase shift (and sensitivity to thickness changes). It should be noted from Fig. 2 that the peaks of the thickness/$\bar{r}$ curves are rather broad and that there is little decrease from optimum sensitivity for twofold variations in the value of $\omega\mu\sigma\bar{r}^2$.

Now let us suppose that we have not yet constructed our coil and can choose $\bar{r}$ to be any value. We can see that the larger we make $\bar{r}$ or the smaller we make thickness/$\bar{r}$, the greater the phase shift. Thus, we

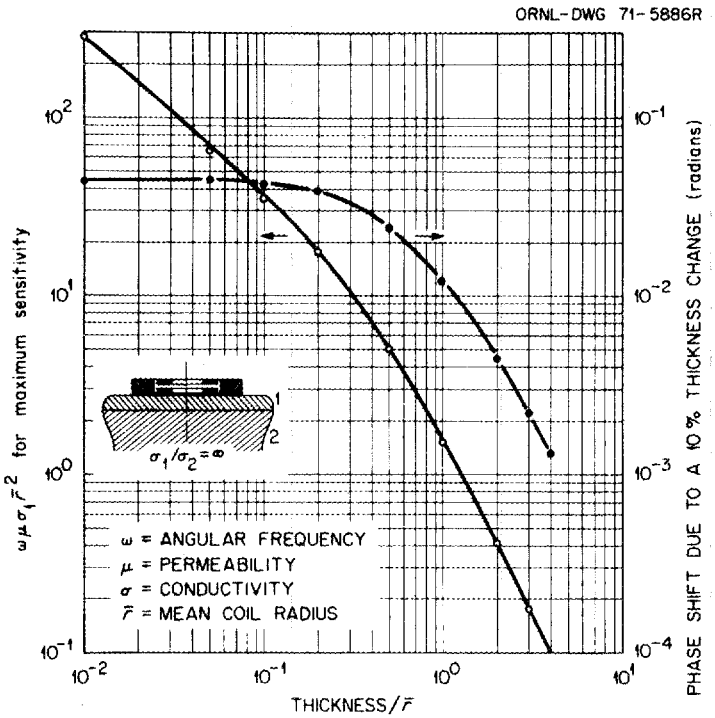

Fig. 3. Value of $\omega\mu\sigma\bar{r}^2$ for Maximum Sensitivity and Phase Shift at Maximum Sensitivity for a 10% Thickness Change Plotted Against Thickness/$\bar{r}$.

are limited only by the area of material we wish to resolve with the coil and by the operating frequency range of our instrument. In general, the larger the coil, the larger the area it samples in one measurement and the lower the operating frequency required for maximum sensitivity. (Although the product of $\omega\mu\sigma\bar{r}^2$ increases as thickness/$\bar{r}$ decreases, it does not increase as fast as $\bar{r}^2$, so therefore ω must decrease.) We also can see that there is very little increase in phase shift for ratios of thickness/$\bar{r}$ of less than 0.2, and that relatively sensitive measurements (1% of the thickness) can be made for ratios as high as 3.

Now that we have succeeded in getting the maximum signal due to thickness changes, we shall take a look at minimizing the effect of the other variables in the problem. The main source of error in any eddy-current test is the lift-off, or coil-to-conductor spacing, and thickness measurements are no exception. For any practical inspection there is a "lift-off range," which is the actual range of spacings encountered when the coil is placed on the specimen. This range extends down to a

"zero lift-off," which is really not zero but a lower bound imposed by such restrictions as insulation thickness. To estimate the error due to lift-off in phase-sensitive eddy-current methods, we calculate the variation in phase shift with lift-off over the lift-off range for instrument settings that bring the error to zero at the extremes of the range. For different values of the inspection parameters the phase shift differs, as shown in Fig. 4. Since we observed that the phase shift could have either sign, as shown by the upper and lower curves, we reasoned that there should be certain conditions where the curves are zero or nearly zero. After some trials with the computer, we discovered that for certain conditions we could get curves such as the middle one in Fig. 4 for $\omega\mu\sigma\bar{r}^2 = 15$. This curve represents the minimum phase shift with lift-off, and the error in the measurement of thickness

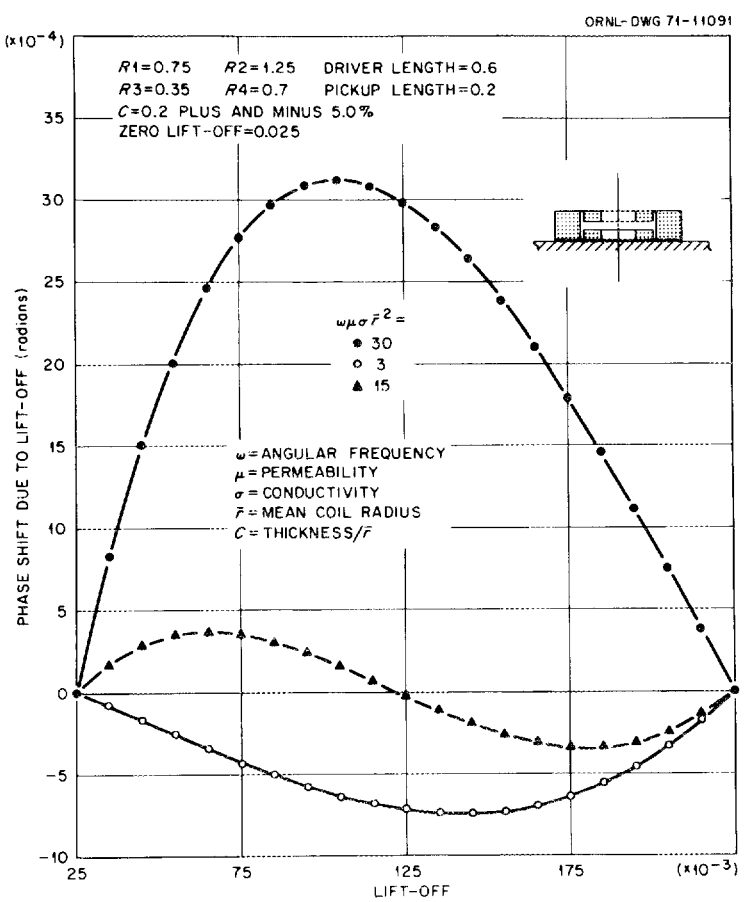

Fig. 4. Plots of Phase Shift Against Lift-Off/$\bar{r}$.

due to this lift-off variation is about 0.15% compared to 1% for the upper and lower curves. (The sensitivity to thickness changes as well as to lift-off is much less in the lower curve.) The value of $\omega\mu\sigma\bar{r}^2$ where this minimum phase shift (induced by lift-off) occurs is a function of the geometry of both the coil and conductor. Figure 5 shows how this value of $\omega\mu\sigma\bar{r}^2$ varies as a function of length of the driver coil for a number of different ratios of thickness to coil mean radius for a zero lift-off equal to $0.05\bar{r}$ and a range of $0.1\bar{r}$.

The optimum value of $\omega\mu\sigma\bar{r}^2$ for the minimum lift-off effect increases considerably as the value of zero lift-off increases. Figures 6 and 7 show curves similar to Fig. 5 for zero lift-off values of 0.025 and $0.1\bar{r}$.

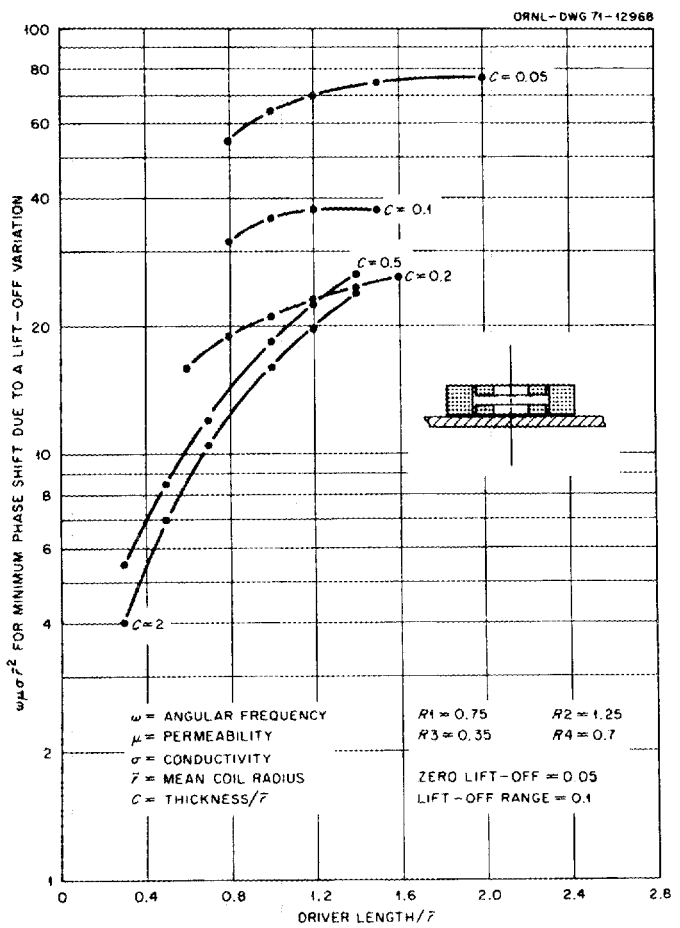

Fig. 5. Value of $\omega\mu\sigma\bar{r}^2$ for Minimum Phase Shift Due to a Lift-Off Variation with Driver Coil Length for Various Values of Nominal Thickness. Zero lift-off $0.05\bar{r}$.

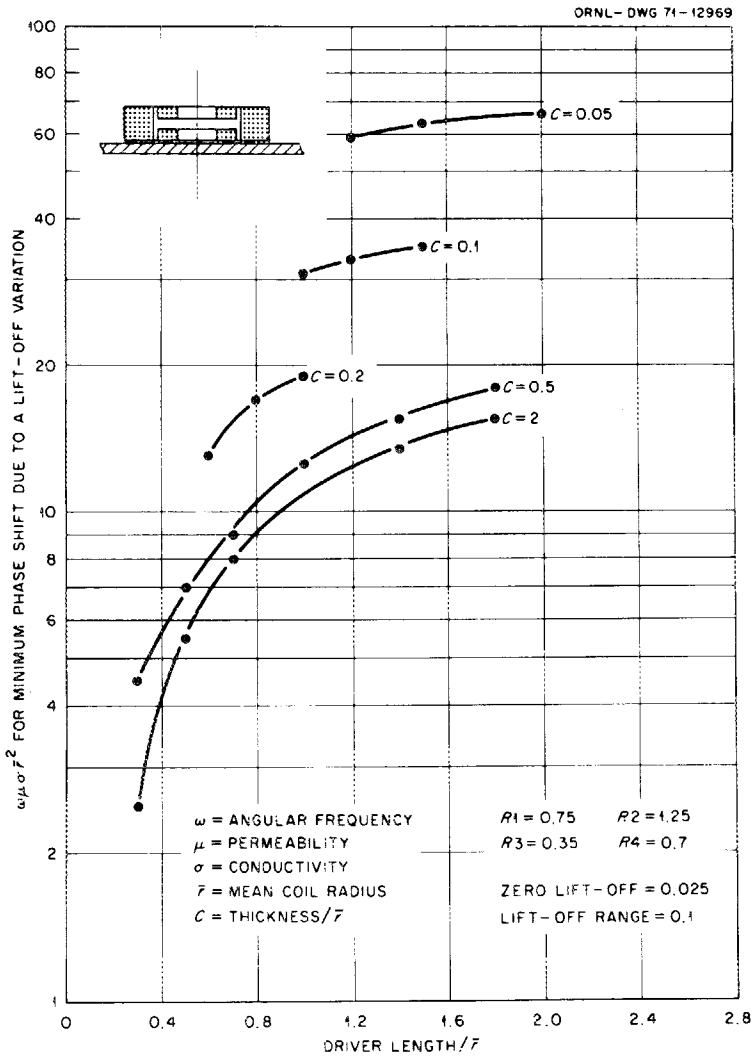

Fig. 6. Value of $\omega\mu\sigma\bar{r}^2$ for Minimum Phase Shift Due to a Lift-Off Variation with Driver Coil Length for Various Values of Nominal Thickness. Zero lift-off $0.025\bar{r}$.

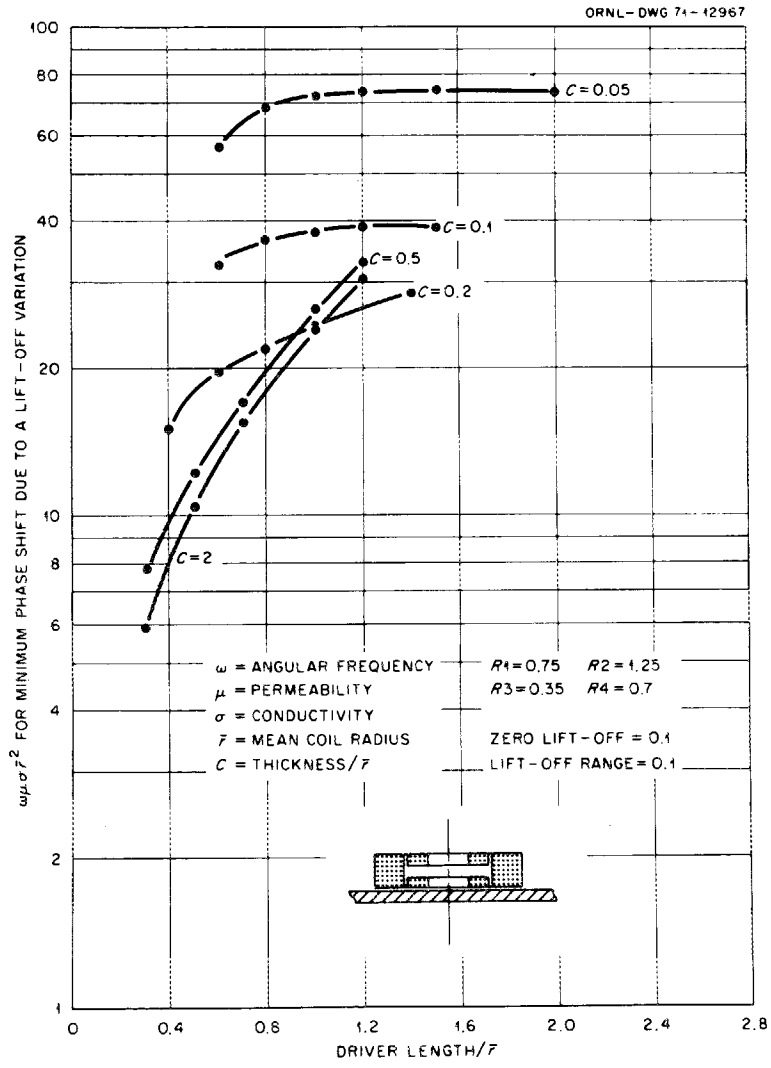

Fig. 7. Value of $\omega\mu\sigma\bar{r}^2$ for Minimum Phase Shift Due to a Lift-Off Variation with Driver Coil Length for Various Values of Nominal Thickness. Zero lift-off $0.1\bar{r}$.

The minimum zero lift-off attainable in practice varies from about $0.025\bar{r}$ for coils having $\bar{r} = 0.4$ in. to $0.1\bar{r}$ for coils having $\bar{r} = 0.02$ in.

The optimum value of $\omega\mu\sigma\bar{r}^2$ for minimum lift-off effect also increases as the lift-off range increases. Figure 8 shows how the optimum value of $\omega\mu\sigma\bar{r}^2$ varies with coil length for lift-off ranges of $0.1\bar{r}$ and $0.2\bar{r}$.

The optimum value of $\omega\mu\sigma\bar{r}^2$ is affected slightly by variations in inner and outer radii of the driver and pickup coils but is relatively independent of the length of the pickup coils. To minimize the effect of lift-off on a thickness measurement, we can choose the coil geometry using Figs. 5 through 8 so that the value of $\omega\mu\sigma\bar{r}^2$ for minimum phase shift due to lift-off is the same as the value of $\omega\mu\sigma\bar{r}^2$ for maximum phase shift due to a 10% thickness change, from Fig. 3.

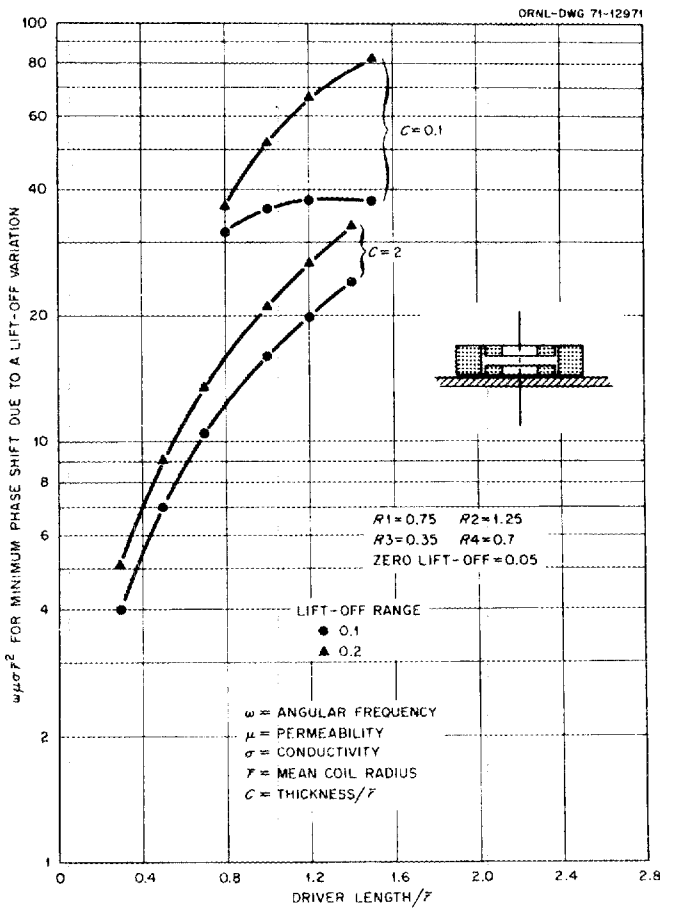

Fig. 8. Value of $\omega\mu\sigma\bar{r}^2$ for Minimum Phase Shift Due to a Lift-Off Variation Plotted Against Driver Coil Length for Various Lift-Off Ranges.

Figure 9 shows how the coil length for minimum lift-off error at the same value of $\omega\mu\sigma\bar{r}^2$ for maximum sensitivity varies as a function of the ratio of thickness to $\bar{r}$, for various values of zero lift-off. Figure 10 shows a similar plot, but with the lift-off range increased from $0.1\bar{r}$ to $0.2\bar{r}$.

Figure 11 shows how the phase shift due to a 10% thickness change and the error in the thickness measurement due to both lift-off variations and conductivity variations change with $\omega\mu\sigma\bar{r}^2$. Thus, for the value of thickness/$\bar{r}$ equal to 0.05, we have been able to choose a coil geometry to minimize the error caused by lift-off variations. The errors in thickness measurements due to lift-off variations of $0.1\bar{r}$ and $0.2\bar{r}$ can be as low as 0.03 and 0.15%, respectively. The 0.03% error due to $0.1\bar{r}$ lift-off variation is in fact below the resolution of the instrument, which is 1.75×10^{-4} radians or 0.05% thickness variation. Having succeeded in significantly reducing the error in measurement due to lift-off, it becomes reasonable to consider the other variables. Figure 11 also shows that an increase of 1% in the conductivity causes the measured value of the thickness to be about 1% high. A conductivity variation of this size could easily be caused by a small change in temperature, local cold working, or heat treatment variations. About the only way to eliminate the error caused by such conductivity variations is to measure the conductivity and correct the thickness readings. Figures 12 through 16 show similar information to Fig. 11 for other values of thickness/$\bar{r}$. From these figures, we can see that the lift-off error can be made minimal by proper selection of coil geometry for thickness/$\bar{r}$ values of 0.1, 0.2, and to some extent 0.5. However, for thicknesses/$\bar{r}$ greater than 0.5, we have reached a practical limit on the "shortness" of our coil and can no longer position the minimum phase shift due to a lift-off variation under the maximum phase shift due to a thickness variation. Because of this fact and the fact that the sensitivity decreases at the higher ratios of thickness/$\bar{r}$, the lift-off error due to a $0.2\bar{r}$ lift-off variation increases to about 1.2% for thickness/$\bar{r}$ equal to 2. (It should be recognized that for a coil even as small as 0.250 in. having a $\bar{r}$ slightly less than 0.125 in., a lift-off variation of $0.2\bar{r}$ would be almost 25 mils, far in excess of that encountered in most practical cases.) The error in thickness measurement

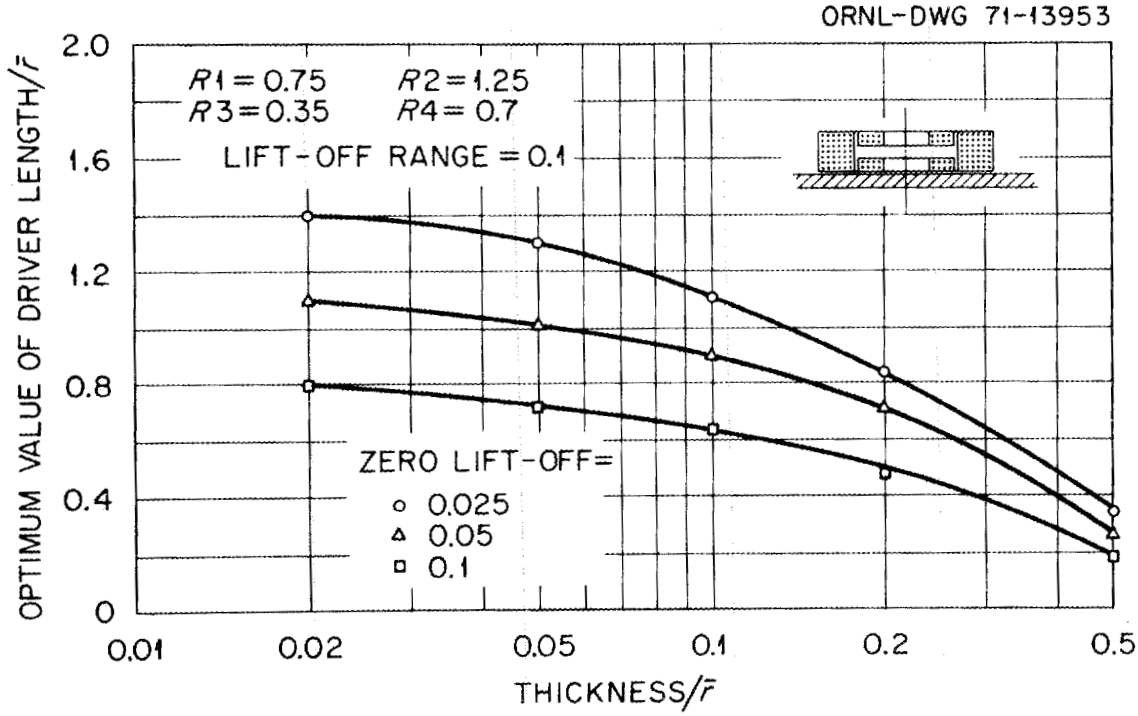

Fig. 9. Optimum Value of Coil Length Plotted Against Nominal Thickness for a Lift-Off Range of $0.1\bar{r}$ for Various Values of Zero Lift-Off.

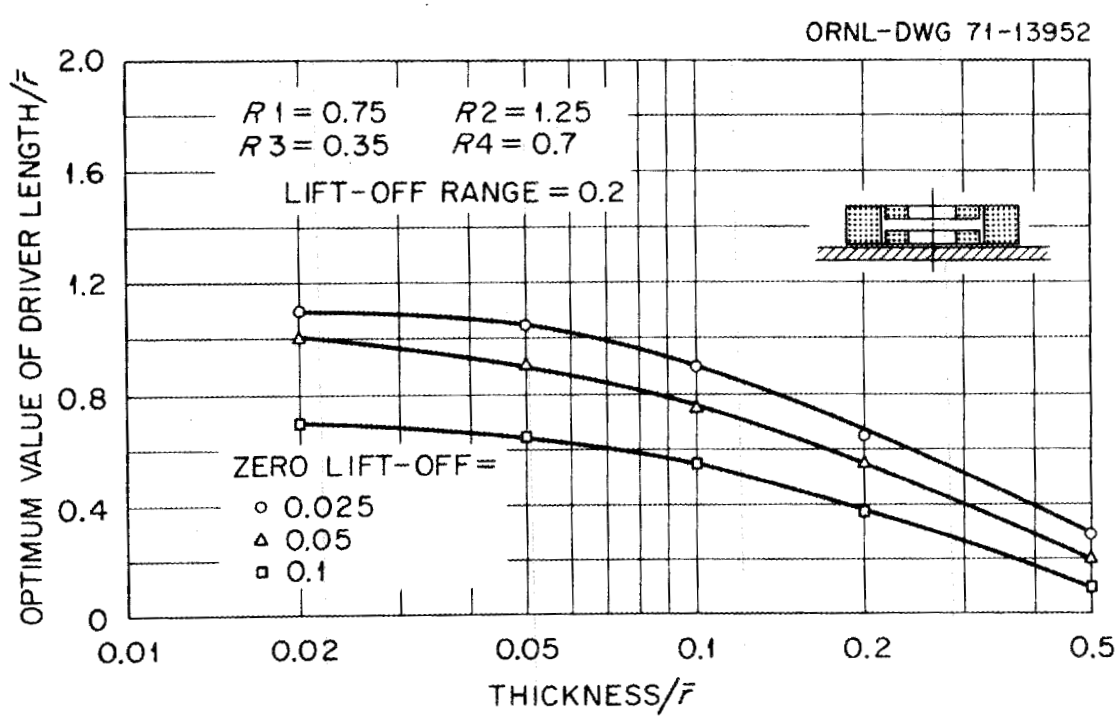

Fig. 10. Optimum Value of Coil Length Plotted Against Nominal Thickness for a Lift-Off Range of $0.2\bar{r}$ for Various Values of Zero Lift-Off.

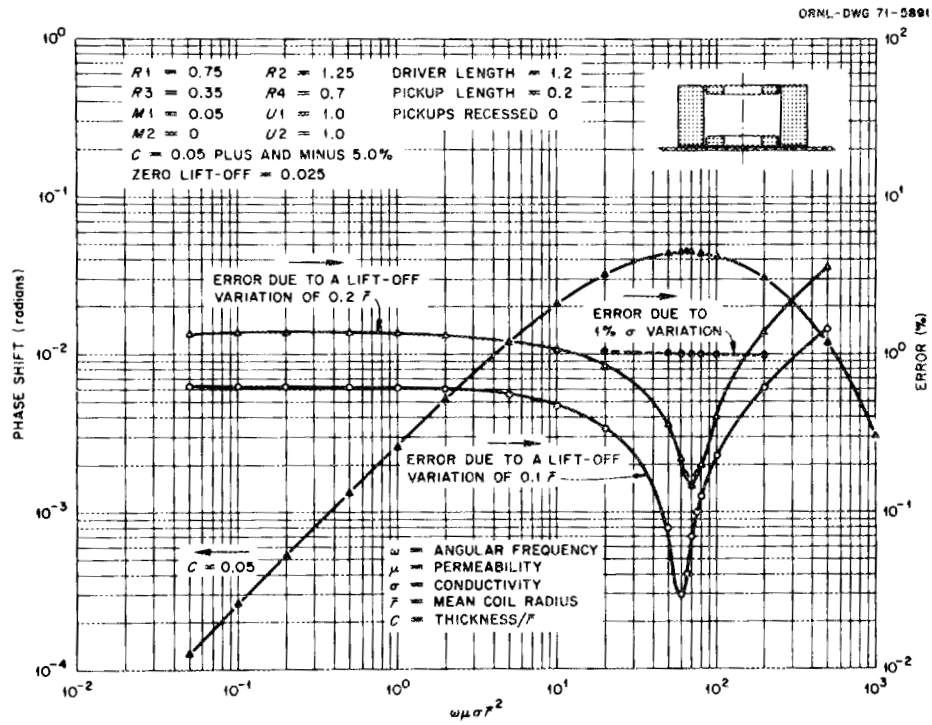

Fig. 11. Phase Shift Due to a 10% Thickness Change and Error in the Thickness Due to Lift-Off Variations and Conductivity Variations Versus $\omega\mu\sigma\bar{r}^2$ for Thickness/$\bar{r}$ Equal to 0.05.

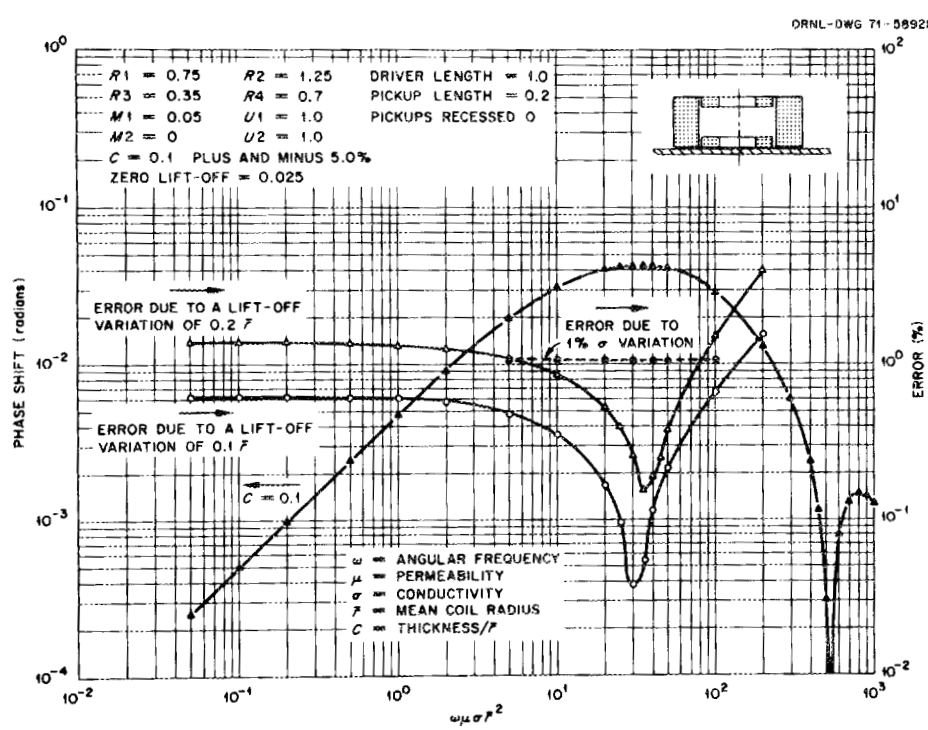

Fig. 12. Phase Shift Due to a 10% Thickness Change and Error in the Thickness Due to Lift-Off Variations and Conductivity Variations Versus $\omega\mu\sigma\bar{r}^2$ for Thickness/$\bar{r}$ Equal to 0.1.

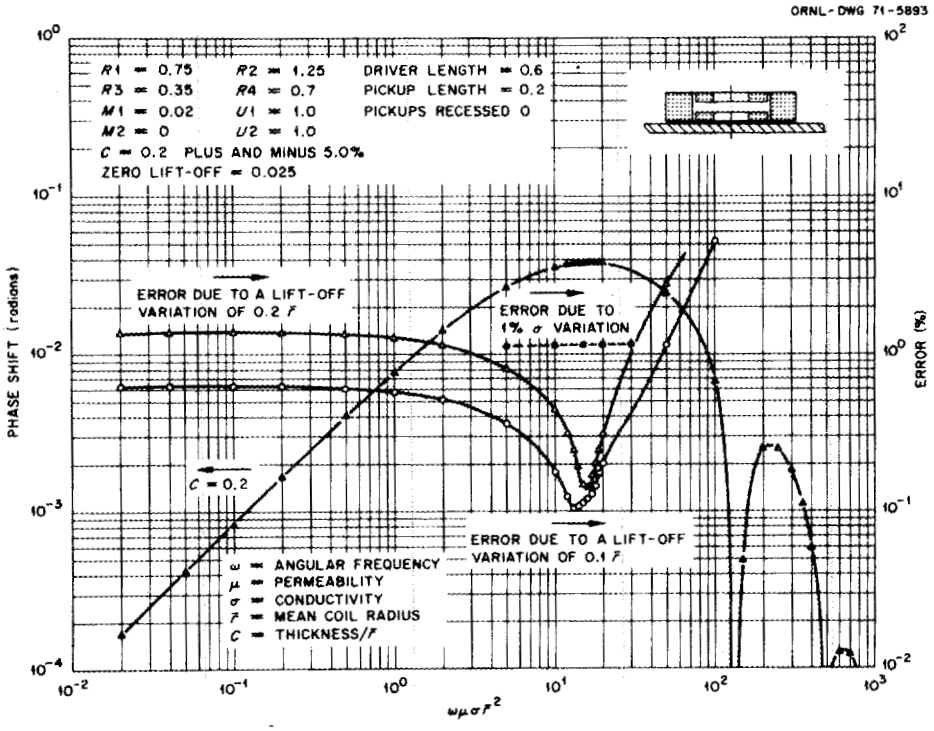

Fig. 13. Phase Shift Due to a 10% Thickness Change and Error in the Thickness Due to Lift-Off Variations and Conductivity Variations Versus $\omega\mu\sigma\bar{r}^2$ for Thickness/$\bar{r}$ Equal to 0.2.

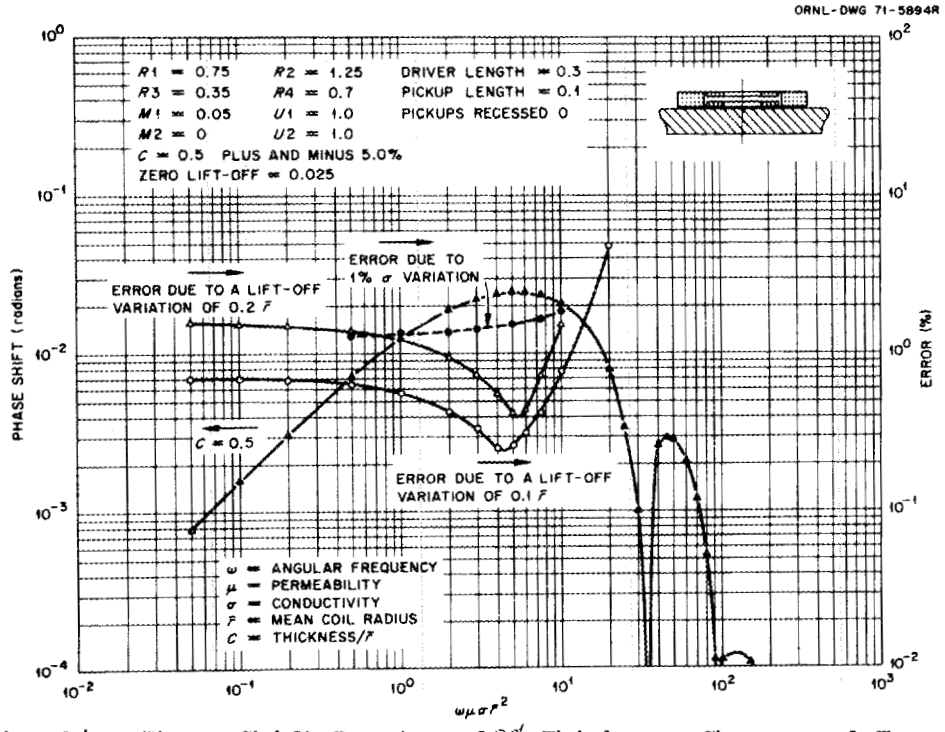

Fig. 14. Phase Shift Due to a 10% Thickness Change and Error in the Thickness Due to Lift-Off Variations and Conductivity Variations Versus $\omega\mu\sigma\bar{r}^2$ for Thickness/$\bar{r}$ Equal to 0.5.

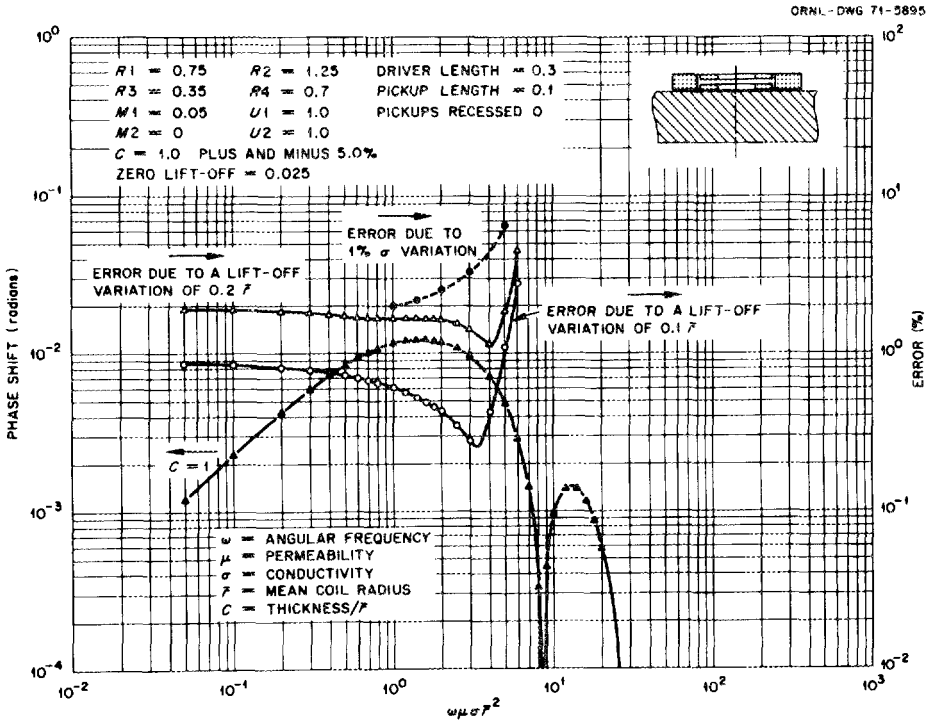

Fig. 15. Phase Shift Due to a 10% Thickness Change and Error in the Thickness Due to Lift-Off Variations and Conductivity Variations Versus $\omega\mu\sigma\bar{r}^2$ for Thickness/$\bar{r}$ Equal to 1.

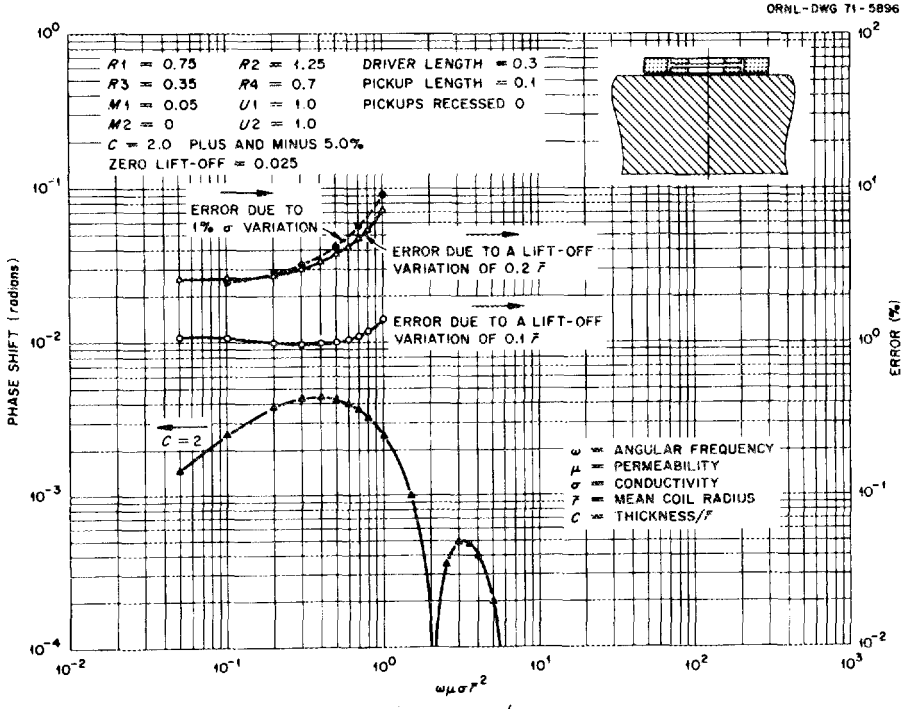

Fig. 16. Phase Shift Due to a 10% Thickness Change and Error in the Thickness Due to Lift-Off Variations and Conductivity Variations Versus $\omega\mu\sigma\bar{r}^2$ for Thickness/$\bar{r}$ Equal to 2.

due to a 1% variation in conductivity increases to about 4% for thickness/$\bar{r}$ equal to 2. Thus, while accurate thickness measurements can be made for ratios of thickness/$\bar{r}$ up to 3, the errors due to variations in conductivity and lift-off can be controlled better at ratios of thickness/$\bar{r}$ of 0.5 and less. The phase shift due to conductivity and thickness variations is quite linear for variations up to 10%. Thus a conductivity or thickness change of 10% would cause 10 times the phase shift of a 1% conductivity or thickness change.

CLADDING THICKNESS MEASUREMENTS

Now that we have studied the special case for a reflection-type coil above a single conductor, we shall consider the thickness measurements of one conductor clad on another.

The sensitivity of the measurement of cladding thickness depends strongly on the ratio of conductivity of the cladding material to the base material. The case of thickness measurements of a single conductor corresponds to cladding thickness measurements with an infinite conductivity ratio, as the base material has zero conductivity. For purposes of discussion let us assume that the base material is 0.1 times as conductive as the cladding material. We have computed curves similar to the ones shown in Fig. 2, showing the phase shift due to a 10% cladding thickness change plotted against $\omega\mu\sigma_1\bar{r}^2$ (σ_1 represents the conductivity of the cladding) for various values of cladding thickness/$\bar{r}$. From these curves we have plotted the value of $\omega\mu\sigma_1\bar{r}^2$ for maximum phase shift and the phase shift for a 10% thickness change against cladding thickness/$\bar{r}$, as shown in Fig. 17. When the conductivity ratio was infinite, as shown in Fig. 3, the phase shift kept increasing as $\bar{r}$ increased (or thickness/$\bar{r}$ decreased). Now, however, the phase shift approaches a rather broad maximum and then decreases. Therefore, we can conclude that there is also an optimum value of the mean radius of the coil for a given nominal cladding thickness. Figures 18 through 21 show similar curves for other conductivity ratios. We can see that there is an optimum value of cladding thickness/$\bar{r}$ for each ratio of conductivity to give a maximum phase shift. Figure 22 shows a plot of this optimum value of cladding thickness/$\bar{r}$

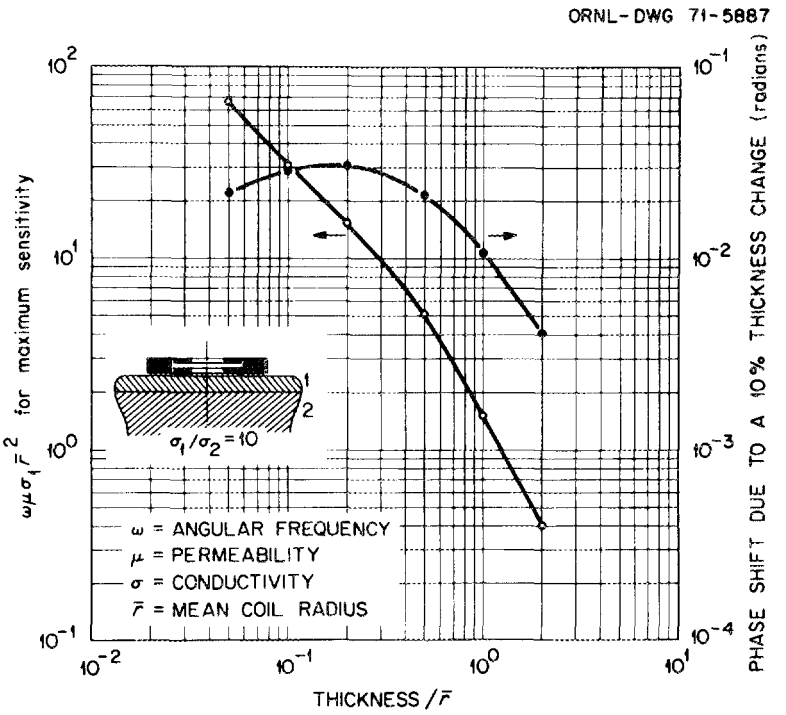

Fig. 17. Value of $\omega\mu\sigma_1\bar{r}^2$ for Maximum Sensitivity and Phase Shift at Maximum Sensitivity for a 10% Cladding Thickness Change Versus Cladding Thickness/$\bar{r}$ for a Conductivity Ratio of 10.

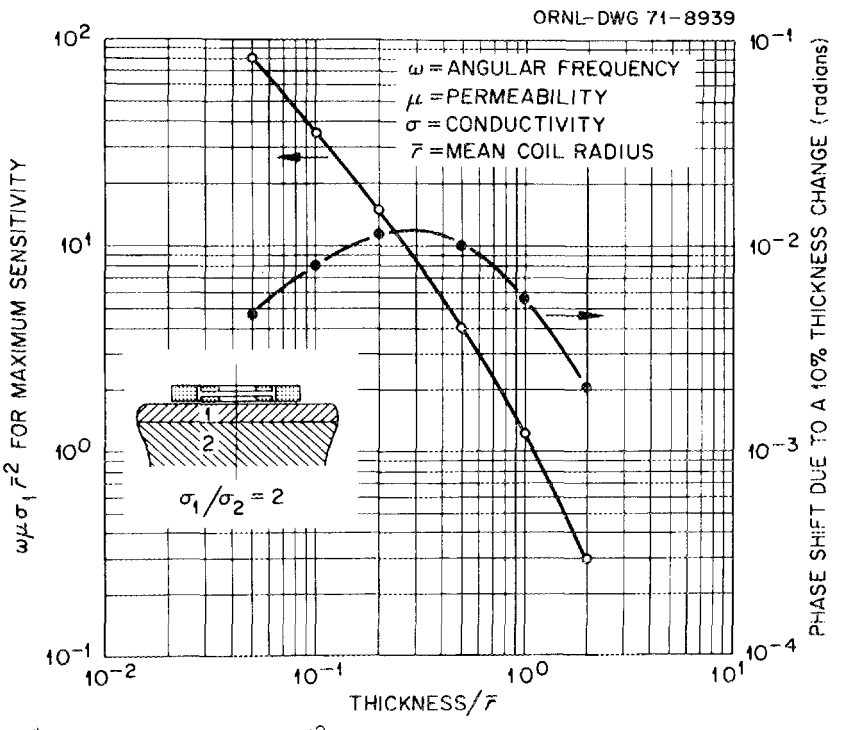

Fig. 18. Value of $\omega\mu\sigma_1\bar{r}^2$ for Maximum Sensitivity and Phase Shift at Maximum Sensitivity for a 10% Cladding Thickness Change Versus Cladding Thickness/$\bar{r}$ for a Conductivity Ratio of 2.

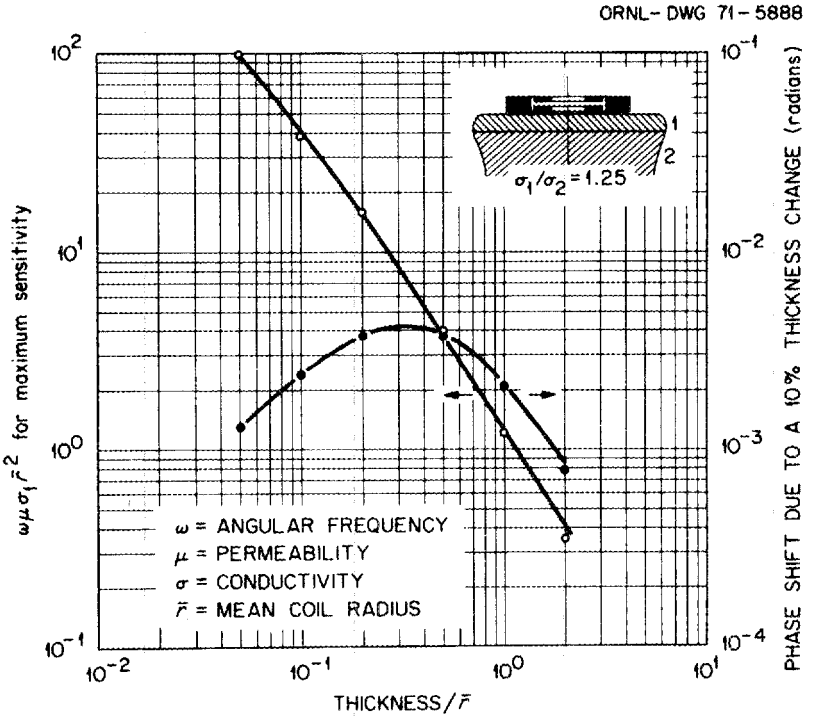

Fig. 19. Value of $\omega\mu\sigma_1\bar{r}^2$ for Maximum Sensitivity and Phase Shift at Maximum Sensitivity for a 10% Cladding Thickness Change Versus Cladding Thickness/$\bar{r}$ for a Conductivity Ratio of 1.25.

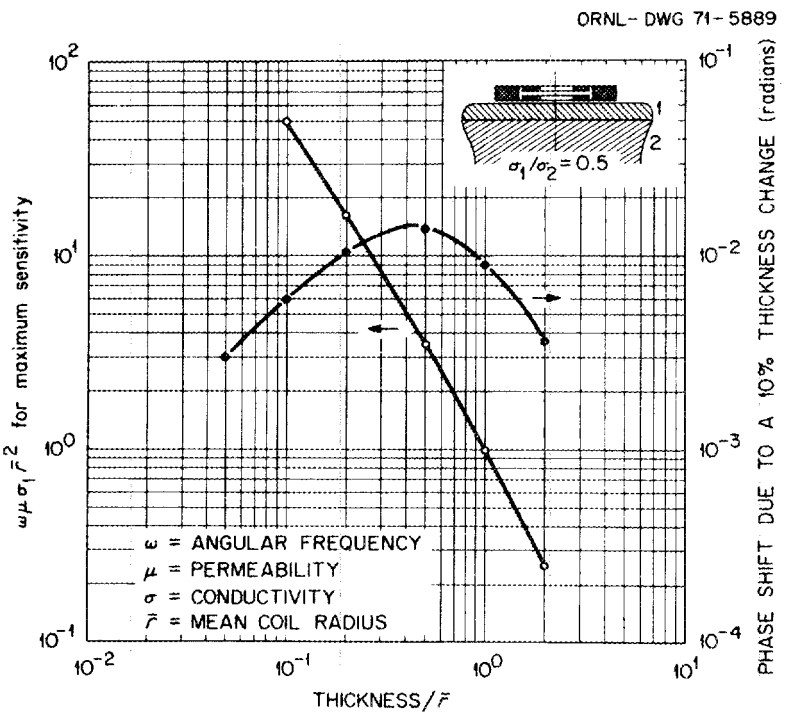

Fig. 20. Value of $\omega\mu\sigma_1\bar{r}^2$ for Maximum Sensitivity and Phase Shift at Maximum Sensitivity for a 10% Cladding Thickness Change Versus Cladding Thickness/$\bar{r}$ for a Conductivity Ratio of 0.5.

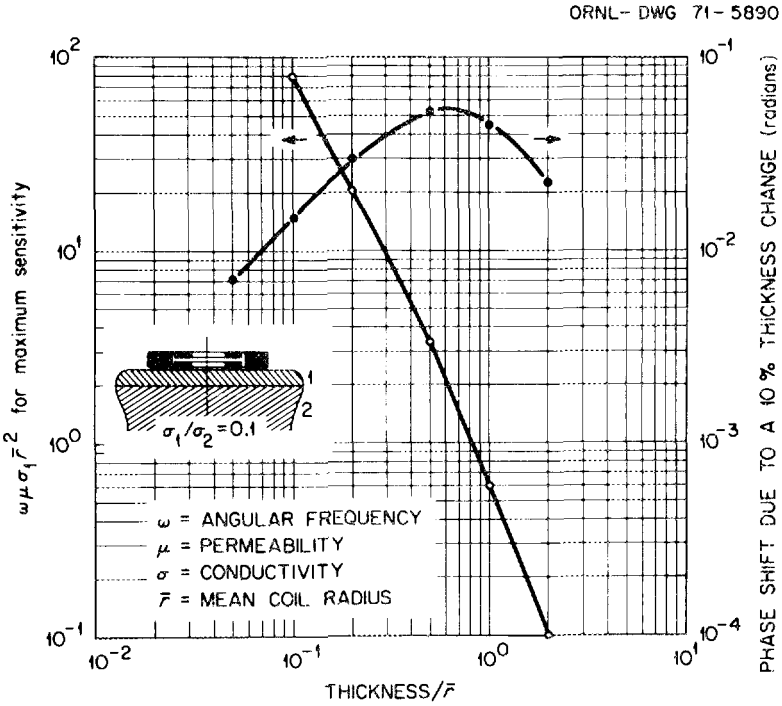

Fig. 21. Value of $\omega\mu\sigma_1\bar{r}^2$ for Maximum Sensitivity and Phase Shift at Maximum Sensitivity for a 10% Cladding Thickness Change Versus Cladding Thickness/$\bar{r}$ for a Conductivity Ratio of 0.1.

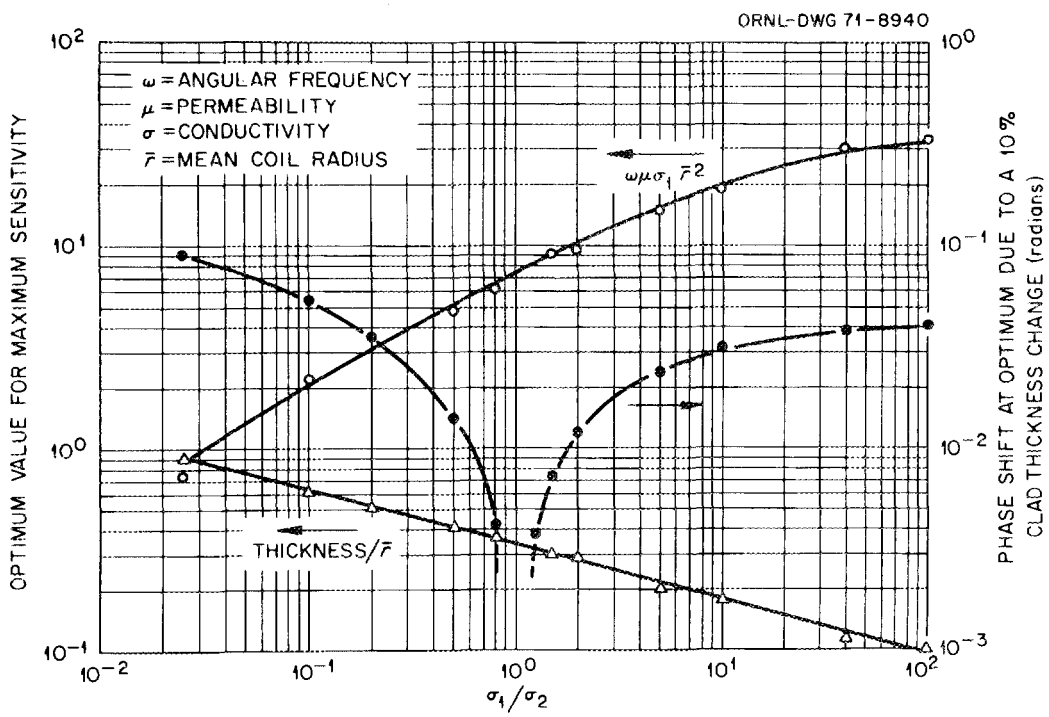

Fig. 22. Value of the Parameters Cladding Thickness/$\bar{r}$ and $\omega\mu\sigma_1\bar{r}^2$ for Maximum Sensitivity and the Phase Shift a Maximum Sensitivity Due to a 10% Change in Cladding Thickness Plotted Against the Ratio of Cladding to Base Material Conductivity.

against the conductivity ratio. In addition, we have also included curves for the optimum value of $\omega\mu\sigma_1\bar{r}^2$ for maximum sensitivity and the phase shift for a 10% cladding thickness change at the maximum sensitivity. From this curve we see that we have adequate sensitivity to measure cladding thickness when the conductivity ratios are as close to 1 as 1.25 or 0.8. (A "rule of thumb" in the past has required conductivity ratios of approximately 2.) Thus, by using optimum parameters, we can measure cladding thickness on materials having conductivities that are almost the same. However, when the materials have exactly the same conductivity, the sensitivity becomes zero.

From Fig. 22 we can determine the optimum size ($\bar{r}$) coil for a given nominal cladding thickness. However, it may be impractical to construct a coil small enough to have the proper cladding thickness/$\bar{r}$ ratio for maximum sensitivity, or if such coil can be constructed, it may take too long to scan a particular specimen with this coil. The curves in Figs. 17 through 21 may be used to show how far away from the optimum value of thickness/$\bar{r}$ we can operate and still have adequate system sensitivity to cladding thickness changes. The curve of phase shift due to a 10% cladding thickness change versus thickness/$\bar{r}$ reaches a rather broad maximum, and the phase shift at one half or twice the optimum thickness/$\bar{r}$ is still approximately 75% of that at the optimum. Likewise, the curve of $\omega\mu\sigma_1\bar{r}^2$ plotted against phase shift reaches a broad maximum, and the exact operating frequency is not critical.

Now that we know how to get maximum (or at least adequate) sensitivity, we shall turn our attention to the elimination of the undesirable variables, starting with lift-off. Figure 23 shows how the length of the driver coil for minimum lift-off error varies as the ratio of σ_1/σ_2 is changed for four values of zero lift-off. The optimum values of thickness/$\bar{r}$ and $\omega\mu\sigma_1\bar{r}^2$ for maximum thickness are used for these curves. Values other than the optimum will require different driver coil lengths to produce the minimum lift-off error. By use of Figs. 22 and 23 we can design coils to have maximum sensitivity to cladding thickness changes and minimum sensitivity to lift-off variations. Figures 24 through 29 show optimally designed coils for measuring cladding thicknesses of materials with different σ_1/σ_2 ratios. All the curves show

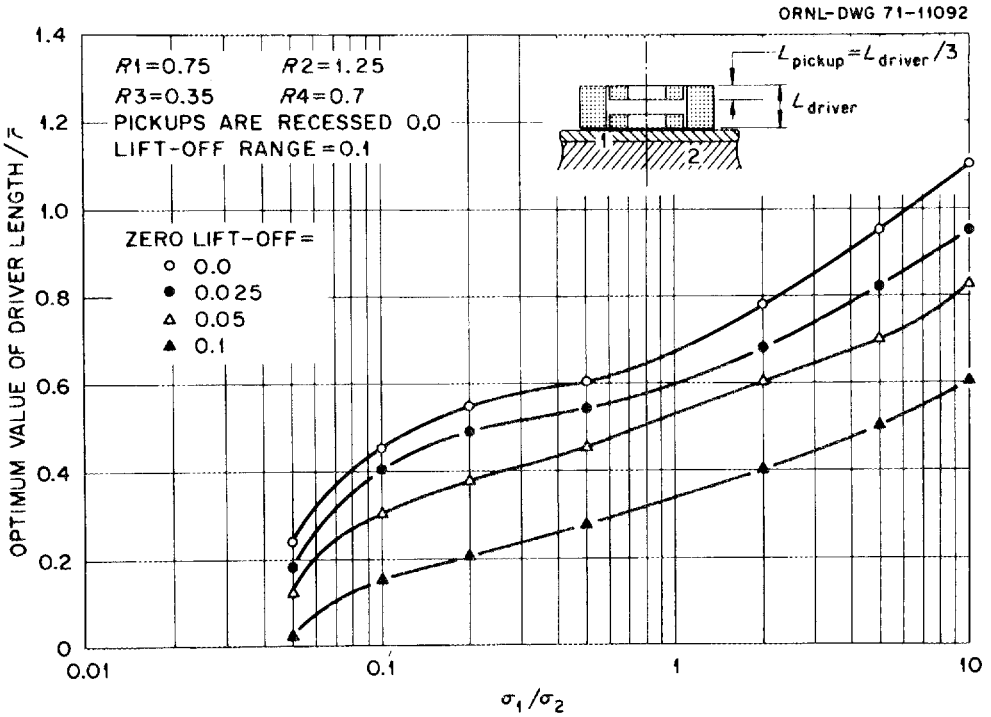

Fig. 23. Value of Coil Length for Minimum Lift-Off-Induced Phase Shift Versus the Ratio of Cladding to Base Material Conductivity.

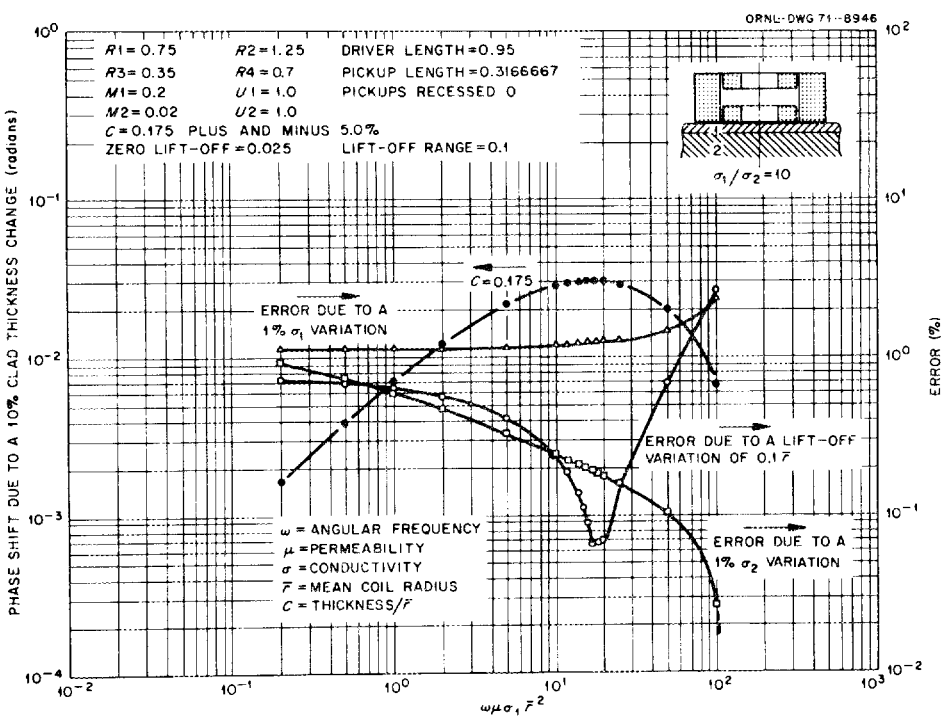

Fig. 24. Phase Shift Due to a 10% Cladding Thickness Change and Error in Cladding Thickness Due to Lift-Off and Conductivity Variations Versus $\omega\mu\sigma_1\bar{r}^2$ for a Conductivity Ratio of 10.

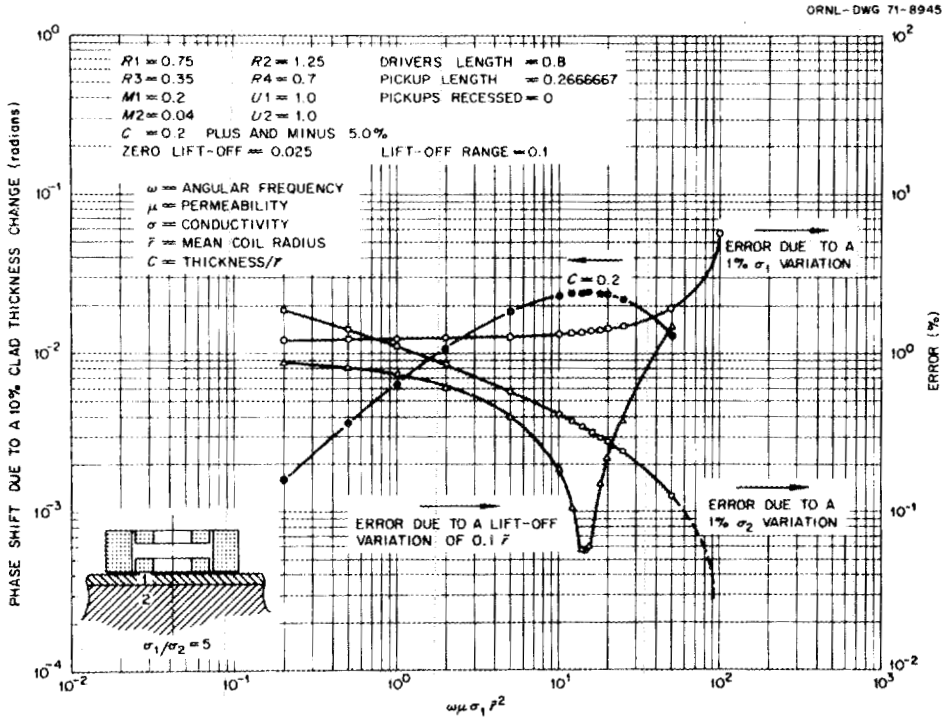

Fig. 25. Phase Shift Due to a 10% Cladding Thickness Change and Error in Cladding Thickness Due to Lift-Off and Conductivity Variations Versus $\omega\mu\sigma_1\bar{r}^2$ for a Conductivity Ratio of 5.

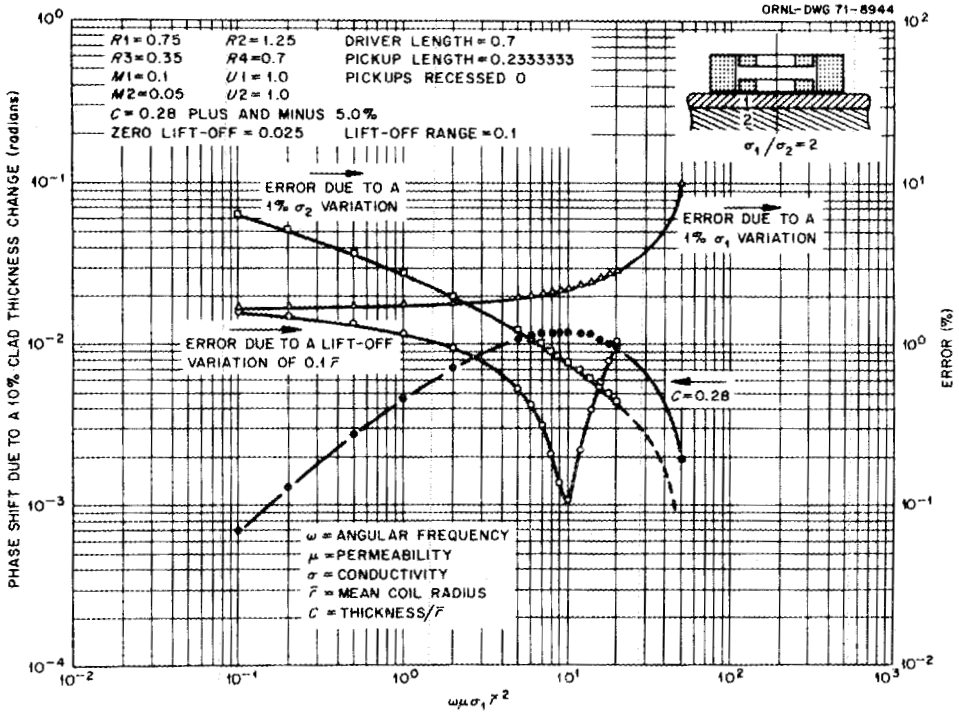

Fig. 26. Phase Shift Due to a 10% Cladding Thickness Change and Error in Cladding Thickness Due to Lift-Off and Conductivity Variations Versus $\omega\mu\sigma_1\bar{r}^2$ for a Conductivity Ratio of 2.

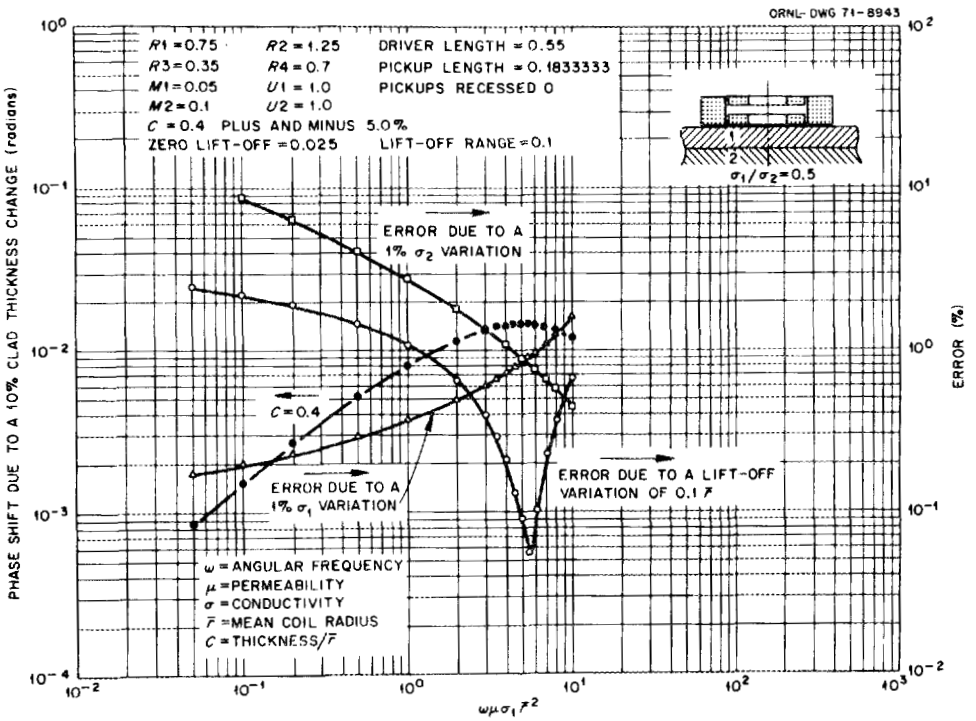

Fig. 27. Phase Shift Due to a 10% Cladding Thickness Change and Error in Cladding Thickness Due to Lift-Off and Conductivity Variations Versus $\omega\mu\sigma_1\bar{r}^2$ for a Conductivity Ratio of 0.5.

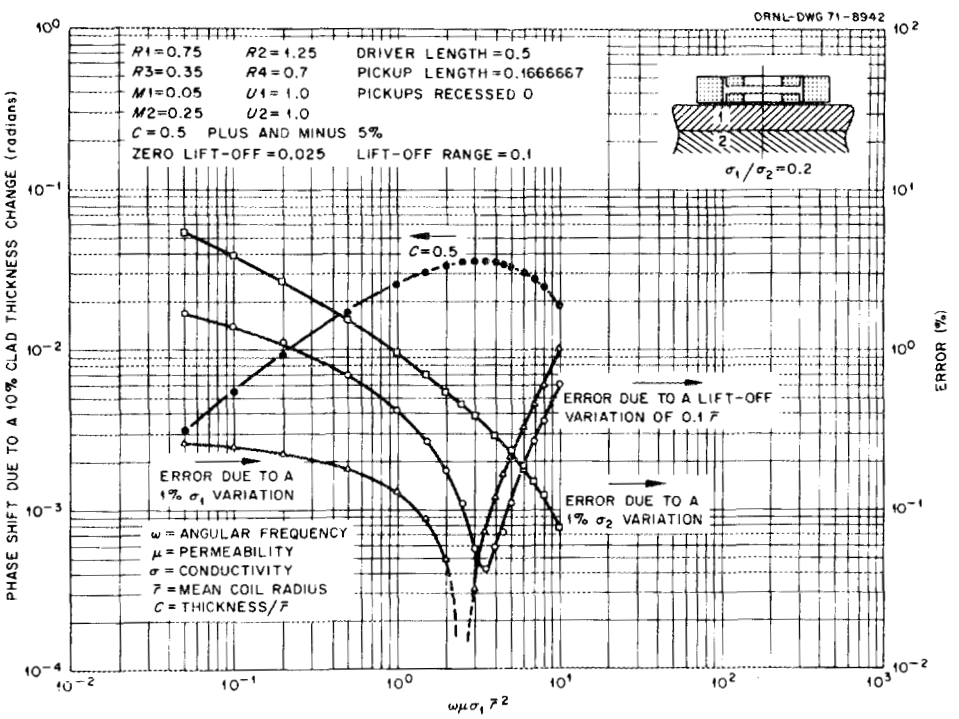

Fig. 28. Phase Shift Due to a 10% Cladding Thickness Change and Error in Cladding Thickness Due to Lift-Off and Conductivity Variations Versus $\omega\mu\sigma_1\bar{r}^2$ for a Conductivity Ratio of 0.2.

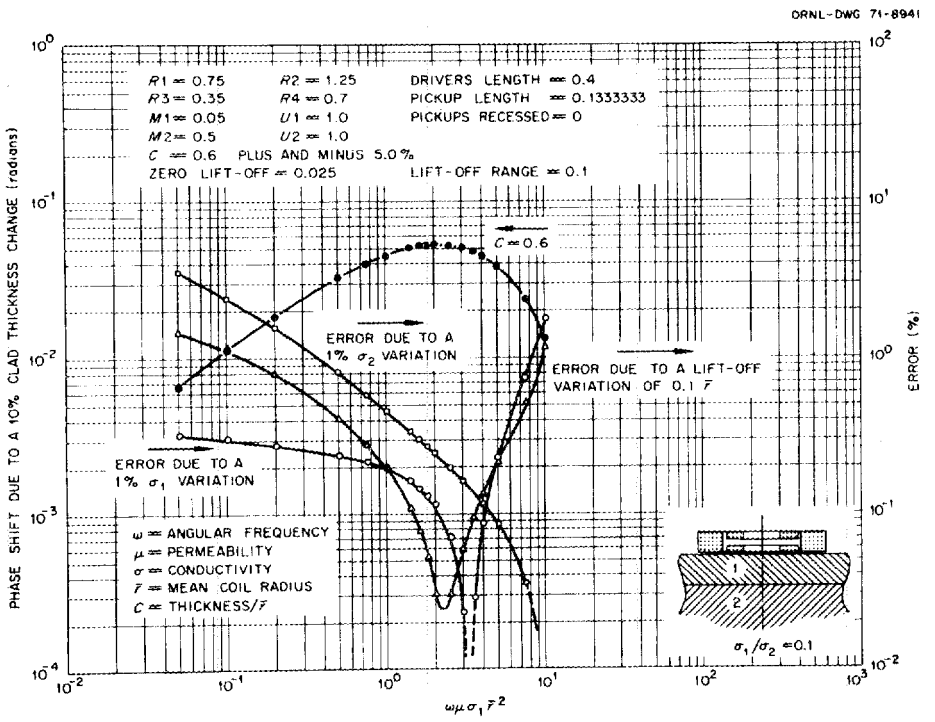

Fig. 29. Phase Shift Due to a 10% Cladding Thickness Change and Error in Cladding Thickness Due to Lift-Off and Conductivity Variations Versus $\omega\mu\sigma_1\bar{r}^2$ for a Conductivity Ratio of 0.1.

a dip in the error due to a lift-off variation of $0.1\bar{r}$ at the same value of $\omega\mu\sigma_1\bar{r}^2$ that produces the maximum phase shift. This dip appears to be somewhat steeper at the lower ratios of σ_1/σ_2, indicating that if the parameters are not properly chosen, the lift-off compensation can cause a decrease in the sensitivity. The error due to a conductivity variation of 1% in either conductor is also given in Figs. 24 through 29.

We can see that the error due to a conductivity variation in the upper conductor, σ_1, is the larger of the two, increases with $\omega\mu\sigma_1\bar{r}^2$, and increases as the σ_1/σ_2 ratio decreases, as long as σ_1 is greater than σ_2. For σ_1 less than σ_2, the σ_1 error is smaller, and for σ_1/σ_2 ratios of 0.2 and 0.1, the σ_1 error becomes quite small. The error due to a variation of 1% in σ_2 becomes largest as the conductivity ratio approaches unity, and decreases as the ratio approaches zero or infinity. The σ_2 error decreases as $\omega\mu\sigma_1\bar{r}^2$ increases. The conductivity and the thickness variations are all fairly linear, up to 10%, so that the amount of phase shift or error can be scaled up or down, depending on the

variation. In principle, multiple frequency operation can be used to eliminate the conductivity errors. One can measure the phase shift at three different frequencies, calculate the conductivity variations, and linearly correct the value of cladding thickness.

PRACTICAL CONSIDERATIONS IN TEST DESIGN

Now we have the knowledge to design the optimum size and shape coil to measure thickness and cladding thickness. Frequently, however, the optimum coil cannot be built, and we must compromise between optimum sensitivity and construction practicality. For instance, the minimum practical size of a coil mean radius, $\bar{r}$, is about 0.015 in. at present. Also, since the effect of lift-off measured in terms of $\bar{r}$ is greater for a smaller coil, such a coil can tolerate less actual lift-off. A lift-off of $0.1\bar{r}$ is equal to 0.040 in. for a 0.4-in.-$\bar{r}$ coil but only 0.0015 in. for a 0.015-in.-$\bar{r}$ coil.

In addition, the resolution of a coil is a direct function of its size. We may wish to make a coil smaller than optimum to increase its sensitivity to thickness changes over a small area or to reduce edge effects. On the other hand, we may wish to make it larger so it will "see" a larger area, thereby increasing the scanning speed. Another reason for operating away from optimum is that we may wish to use an existing coil for a new problem.

Although many of the curves given in this report are for optimum conditions, it is not critical that we operate at optimum. In general, the curves for optimum sensitivity have rather broad peaks, and if the operating conditions differ by a factor of 0.5 to 2 from the optimum parameters, we will still have about 75% of the maximum sensitivity.

The actual circuit parameters, as shown in Fig. 30, also have an effect on the phase shift. All phase shifts given thus far have been for an infinite input impedance to the driver coil and an infinite load impedance in the pickup coil. (This condition requires that the shunt capacitance in the driver and pickup circuits be zero.) Then the phase shift depends only on the mutual coupling and is independent of the number of turns on each coil. However, since we cannot achieve infinite

ORNL-DWG 72-671

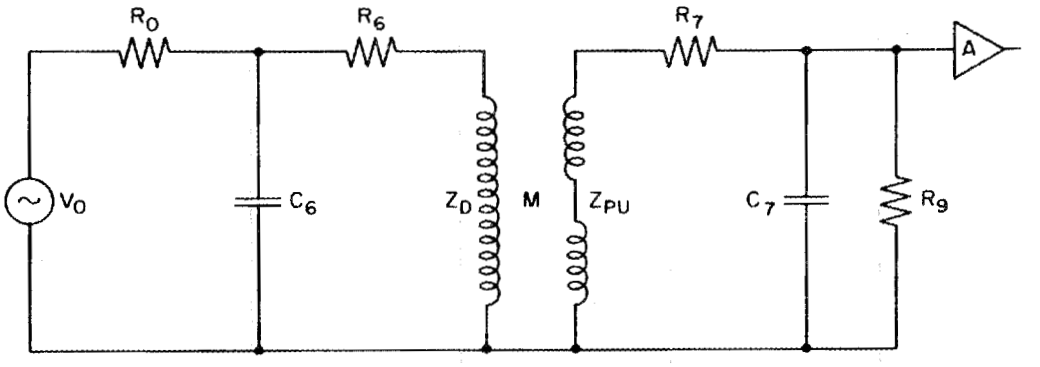

V_0 DRIVING VOLTAGE
R_0 SERIES RESISTANCE IN THE DRIVING CIRCUIT
C_6 SHUNT CAPACITANCE OF THE DRIVING CIRCUIT
R_6 D.C. RESISTANCE OF THE DRIVER COIL
Z_D IMPEDANCE OF THE DRIVER COIL
M MUTUAL IMPEDANCE BETWEEN THE DRIVER AND PICK-UP COILS
Z_{PU} IMPEDANCE OF THE PICK-UP COILS
R_7 D.C. RESISTANCE OF THE PICK-UP COILS
C_7 SHUNT CAPACITANCE OF THE PICK-UP CIRCUIT
R_9 AMPLIFIER INPUT IMPEDANCE

Fig. 30. Simplified Circuit Diagram for an Eddy-Current Reflection-Type Probe.

impedances in actual practice, we must consider the entire circuit of the probe. In general, if we have designed the probe circuit properly, we will get the following desirable results:

1. The R-L-C circuit will limit the frequency response of the probe and reduce noise.

2. The phase shift due to changes in the coils' dc resistance can be completely eliminated, thus drastically reducing temperature drift in the probe.

3. By varying the values of R, L, and C in the circuit, we can vary the value of $\overline{r}^2\omega\mu\sigma$ where the minimum lift-off effect occurs after the coil has been constructed.

In general, for a properly designed R-L-C circuit, the change in phase shift and sensitivity from the ideal case of infinite source and load impedance is about 2% or less. A computer program (RFCLAD) to

design the actual probe circuit and to calculate the response of a probe away from optimum conditions is given in another report.[8]

EXAMPLES OF DESIGN AND EXPERIMENTAL RESULTS

We shall now consider three examples of the design of eddy-current tests. These examples were chosen because we had six probes that were identical except for constructional variations. By having six probes available, we could statistically analyze the results, including consideration of the constructional variations. These tests were actually designed to fit the probes, but we shall now proceed to design the probes to fit these tests.

The first problem we shall consider is the design of a test to measure the thickness of aluminum alloy 7075 ($\rho = 3.755$ $\mu\Omega$-cm) in the range of 0.075 to 0.085 in. with a nominal value of 0.080 in. From Fig. 3 on p. 5, we see that there is no optimum size coil, and, as long as the ratio of thickness/$\bar{r}$ is less than 0.5, the coils will be fairly sensitive. Also, from Fig. 9 on p. 11 we see that we can effectively reduce sensitivity to lift-off variations if the ratio is less than 0.5. We therefore choose a coil mean radius of 0.300 in. (largely because of its availability), which gives a ratio of thickness/$\bar{r}$ = 0.267. From Fig. 3 we see that the optimum value of $\omega\mu\sigma\bar{r}^2$ for this ratio is about 13 and the sensitivity to a 10% thickness change is 0.035 radians or 2.0°. The value of $\omega\mu\sigma\bar{r}^2$ is given in MKS units, but we can use the following conversion factor and use more familiar units. We can write $\omega\mu\sigma\bar{r}^2 = 0.51 \times F \times \bar{r}^2/\rho$, where F is the frequency in Hertz, $\bar{r}$ is in inches, and ρ is the resistivity in microhm centimeters. Solving the above equation gives

$$13 = 0.51 \times F \times (0.3)^2/3.755 ,$$

or

$$F = 13 \times 3.755/(0.09 \times 0.51) = 1.06 \text{ kHz}.$$

---

[8]C. V. Dodd and C. C. Cheng, The Analysis of Reflection-Type Coils for Eddy-Current Testing, report in preparation.

We chose 1 kHz as the actual operating frequency. The sensitivity for a 10% thickness change is 2.0°, and the sensitivity for the 12.25% thickness change for the actual range of 0.0755 to 0.0853 in. is 2.45°. The more accurate calculation performed by the computer program RFCLAD gave a phase shift of 2.43° for the stated thickness variation. The experimental measurements gave an average phase shift of 2.41° for the six coils, with a standard deviation of 0.08°.

The error between calculated and measured sensitivity was 0.02° or 0.8%. The average of the experimental phase shift is plotted against thickness in Fig. 31. The thickness of the curve represents the variation caused by lift-offs from 0 to 0.030 in. The maximum variation in phase due to the lift-off variation is 0.05° measured, compared to 0.045° calculated. This phase shift is difficult to measure because it is not much larger than the instrumental resolution.

The next problem we shall consider is the design of a test to measure the thickness of aluminum alloy 7075 over the range 0.110 to 0.130 in., with a nominal thickness of 0.120 in. Again, using a coil mean radius of 0.300 in. gives a thickness/$\bar{r}$ ratio of 0.4. From Fig. 3 we see that

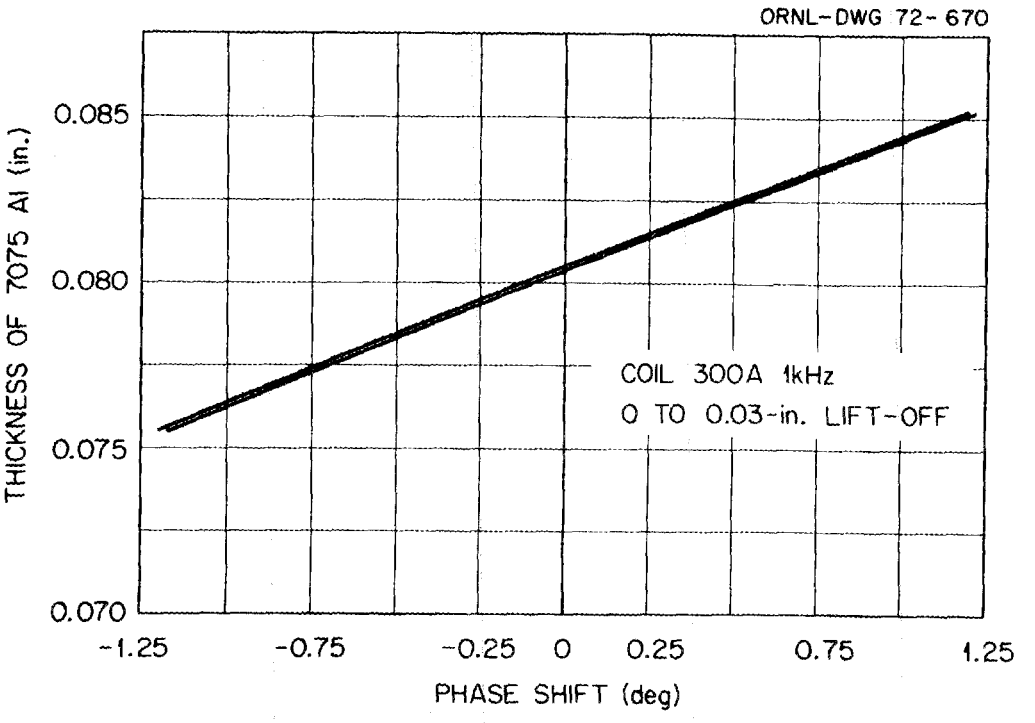

Fig. 31. Phase Shift Versus Thickness for a 300 Å Coil at 1 kHz with 0 to 0.030-in. Lift-Off Variation.

the optimum value of $\bar{r}^2\omega\mu\sigma_1$ for maximum sensitivity is 7, and the sensitivity for a 10% thickness change is 0.028 radians or 1.60°. Solving for the test frequency gives:

$$7 = 0.51 \times F \times (0.3)^2/3.755 \quad ,$$

or

$$F = 7 \times 3.755/(0.09 \times 0.51) = 573 \text{ Hz}.$$

We chose 500 Hz as the actual operating frequency. The sensitivity read from the curves is 1.60° for a 10% thickness change, or 2.62° for the 16.3% thickness change for the actual range from 0.1108 to 0.1304 in. The more accurate calculations performed by the computer program RFCLAD gave a phase shift of 2.80°. The average of the experimental measurements for the six coils was 2.84°, with a standard deviation of 0.07°. The difference between the calculated and measured sensitivity was 0.04° or 1.4%. The phase shift due to a lift-off change from 0 to 0.030 in. was 0.07° for both the calculations and measurements.

The final case we shall consider is the design of a test to measure 0.075 to 0.085 in. of aluminum alloy 7075 (ρ = 3.755 $\mu\Omega$-cm) clad on nickel-copper alloy (ρ = 9.65 $\mu\Omega$-cm). The ratio of the conductivities is 2.57, and from Fig. 22, p. 16, we find that the optimum ratio of thickness/$\bar{r}$ is 0.26. Since the nominal thickness is 0.080 in., we then calculate the coil mean radius to be $\bar{r}$ = 0.080 in./0.26 = 0.307 in., and we therefore choose $\bar{r}$ = 0.300. From Fig. 22 we see that the value of $\bar{r}^2\omega\mu\sigma_1$ for maximum sensitivity is 13 and the sensitivity for a 10% cladding thickness change is 0.015 radians or 0.86°.

The operating frequency is calculated to be F = 13 × 3.755/(0.09 × 0.51) = 1.06 kHz, so we choose 1 kHz as the operating frequency. The sensitivity of 0.86° as read from Fig. 22 for a 10% thickness variation corresponds to a sensitivity of 1.05° for the actual 12.25% cladding thickness variation. The more accurate calculation made by the computer program RFCLAD gives 1.04°. The average of the experimental measurements for five coils was 0.99° with a standard deviation of 0.03°. The error between calculated and measured sensitivity is 0.05° or 5%. The variation due to lift-off was 0.04° for both the calculations and the measurements.

These three cases indicate how we can design coils for thickness and cladding thickness measurements. If the coils had not been previously constructed, we would have also varied the coil length according to Figs. 9, 10, and 23 to minimize the lift-off effects.

A number of other coils have been designed and tested. Thicknesses ranging from 0.0002 to 0.6 in. have been measured with frequencies ranging from 120 Hz to 5 MHz and resistivities ranging from 1.7 to 1000 μΩ-cm. The accuracy of the measurements was in most cases within 10% of the estimated and calculated values, which were always within experimental error.

SUMMARY AND CONCLUSIONS

The curves presented in this report allow a quick and accurate method of designing eddy-current tests and eddy-current coils. They also help apply existing coils more intelligently to inspection problems, allow rapid feasibility studies to be made, show the effects of undesirable variables, and provide the starting point for more accurate calculations, which can be made with the computer program RFCLAD.

These curves and the experimental measurements show that very accurate eddy-current tests can be applied to a much greater range of thickness and cladding thickness measurements than previously believed possible.

ACKNOWLEDGMENTS

The authors would like to acknowledge L. D. Chitwood and O. E. Conner for performing the measurements, S. Petersen for editing, and Sharon Woods for typing the manuscript.

INTERNAL DISTRIBUTION

1–3. Central Research Library
4. ORNL – Y-12 Technical Library
Document Reference Section
5–14. Laboratory Records Department
15. Laboratory Records, ORNL RC
16. ORNL Patent Office
17. G. M. Adamson, Jr.
18. D. A. Canonico
19. G. W. Clark
20. F. L. Culler
21. J. E. Cunningham
22–101. C. V. Dodd
102. J. H Frye, Jr.
103. W. Fulkerson
104. J. W. Garber (Y-12)
105. W. O. Harms
106–108. M. R. Hill
109. C. C. Lu
110. D. L. Mason (Y-12)
111. R. W. McClung
112. F. D. Mundt (Y-12)
113. H. C. Schweinler
114. G. M. Slaughter
115. W. A. Simpson
116. D. B. Trauger
117. J. R. Weir, Jr.

EXTERNAL DISTRIBUTION

118. S. Aveyard, AERE-Harwell, Didcot, Berkshire, England
119. Robert W. Bailey, Jr., WRAMA/MMETM, Service Engineering, Robbins Air Force Base, GA 31093
120. Robert A. Baker, Sandia Corporation, Division 7361, P.O. Box 5800, Albuquerque, NM 87115
121. D. W. Ballard, Sandia Corporation, Division 7361, P.O. Box 5800, Albuquerque, NM 87115
122. Carl E. Baum, Kirtland Air Force Base, NM 87115
123. Harold Berger, Metallurgy Division, Argonne National Laboratory, 9700 S. Cass Avenue, Argonne, IL 60439
124. Benard Boisvert, SAAMA/MMEW, Kelly Air Force Base, TX 78241
125. R. L. Brown, Jr., WADCO Corporation, P.O. Box 1970, Richland, WA 99352
126. R. L. Caryl, LTV Electrosystems, Inc., Commercial Services Division, P.O. Box 1056, Greenville, TX 75401
127. John Carlyle, MAMM-14, Naval Air Development Center, Johnsville, Warminster, PA 18974
128–129. E. G. Case, Director, Division of Reactor Standards, AEC, Washington, DC 20545
130. C. C. Cheng, Physics Department, Northwestern College, Orange City, IA 51041
131. D. F. Cope, RDT, SSR, AEC, Oak Ridge National Laboratory
132. F. L. Crestridge, ARA-3, Aerojet Nuclear Corporation, P.O. Box 1845, Idaho Falls, ID 83401
133. W. E. Deeds, The University of Tennessee, Knoxville, TN 37900
134. N. B. Edenborough, Los Alamos Scientific Laboratory, P.O. Box 1663, Los Alamos, NM 87544

135. D. Elliott, Los Alamos Scientific Laboratory, P.O. Box 1663, Los Alamos, NM 87544
136–140. Executive Secretary, Advisory Committee on Reactor Safeguards, AEC, Washington, DC 20545
141. Robert F. Feldman, General Electric Company, Route I-75, Maildrop E-45, Evendale, OH 45215
142. John H. Flora, Battelle Memorial Institute, Columbus, OH 43201
143. Ronald Frailer, Physical Laboratory Branch, Inspection Operations Division, Quality Assurance Directorate, Edgewood Arsenal, MD 21010
144. John Gleim, Naval Ship Engineering Center, Hyattsville, MD 20782
145. A. J. Glispin, Department 84-35, Lockheed Missiles and Space Company, Sunnyvale, CA 94086
146. Robert C. Grubinskas, Department of the Army, Army Materials and Mechanics Research Center, Watertown, MA 02172
147. Donald L. Green, WADCO Corporation, P.O. Box 1970, Richland, WA 99352
148. John Haynes, Federal Electric Corporation, 2109 Clinton Avenue, W., Huntsville, AL 35805
149. H. R. Huxford, Savannah River Plant, E. I. du Pont de Nemours and Company, Aiken, SC 29801
150. R. H. Jungers, HQ. AFLC/MAFT, Wright-Patterson Air Force Base, OH 45433
151. D. L. Lessor, Battelle-Northwest, P.O. Box 999, Richland, WA 99352
152. H. L. Libby, Battelle-Northwest, P.O. Box 999, Richland, WA 99352
153. L. A. Lott, Dow Chemical Company, Rocky Flats Division, P.O. Box 888, Golden, CO 80401
154. C. L. Matthews, RDT, OSR, AEC, Oak Ridge National Laboratory
155. M. C. McIlwain, R-QUAL-ARA, G. C. Marshall Space Flight Center, Marshall Center, AL 35812
156. Charles P. Merhib, NDT Information Analysis Center, Army Materials and Mechanics Research Center, Watertown, MA 02172
157–159. Peter A. Morris, Director, Division of Reactor Licensing, AEC, Washington, DC 20545
160. Roy Nance, Westinghouse Bettis Atomic Power Laboratory, P.O. Box 79, West Mifflin, PA 15122
161. H. Pederson, WADCO Corporation, P.O. Box 1970, Richland, WA 99352
162. J. F. Pierce, The University of Tennessee, Knoxville, TN 37900
163. Dennis Rathbun, Sandia Corporation, P.O. Box 969, Livermore, CA 94550
164. C. J. Renken, Argonne National Laboratory, 9700 S. Cass Avenue, Argonne, IL 60439
165. R. R. Rowand, Hq. AFML/LLN, Wright-Patterson Air Force Base, OH 45433
166. Roy S. Sharpe, AERE-Harwell, Didcot, Berkshire, England
167. Carl B. Shaw, WADCO Corporation, P.O. Box 1970, Richland, WA 99352
168. Sidney Siegel, Atomics International, P.O. Box 309, Canoga Park, CA 91304
169. J. M. Simmons, AEC, Washington, DC 20545

170. E. E. Stansbury, The University of Tennessee, Department of Metallurgical Engineering, Knoxville, TN 37900
171. Harold Stevens, Hq. AFML/MAMN, Wright-Patterson Air Force Base, OH 45433
172. Gerald C. Stoker, Sandia Corporation, Division 7361, P.O. Box 5800, Albuquerque, NM 87115
173. F. E. Thompson, Chief, Physical Laboratory Branch, Quality Assurance Directorate, Edgewood Arsenal, MD 21010
174. Alex Vary, NASA-Lewis Research Center, 21000 Brookpark Road, Cleveland, OH 44135
175. D. L. Waidelich, Department of Electrical Engineering, University of Missouri, Columbia, MO 65201
176. J. K. White, Westinghouse Research and Development, Pittsburgh, PA 15235
177. Laboratory and University Division, AEC, Oak Ridge Operations
178–179. Division of Technical Information Extension